Supporting Information

Hyodo et al. 10.1073/pnas.1113106108

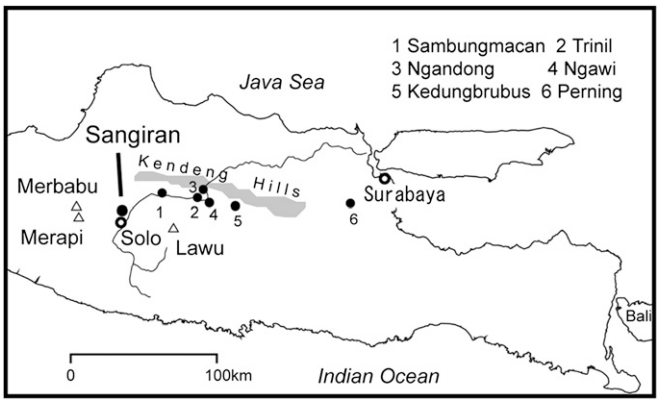

Fig. S1. Map of Central and East Java. Solid circles show hominid fossil sites of Sangiran, Sambungmacan, Trinil, Ngandong, Ngawi, Kedungbrubus, and Pernning (Mojokerto).

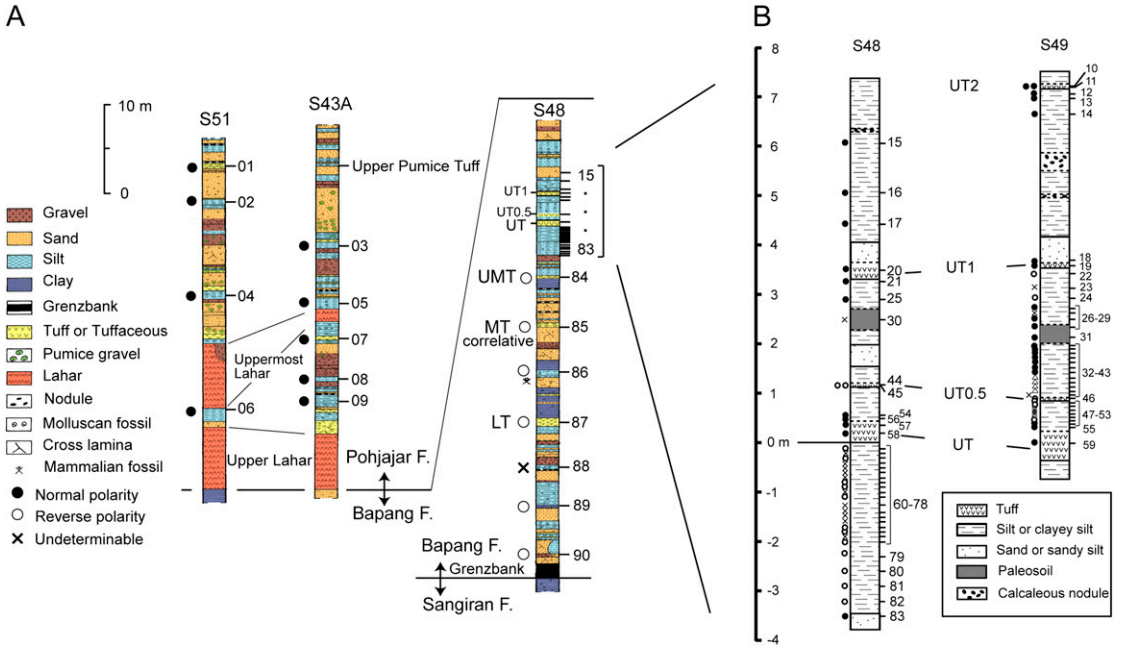

Fig. S2. Stratigraphic levels of paleomagnetic samples. (*A*) Lithostratigraphy of the Pohjajar and Bapang Formations. (*B*) Lithostratigraphy around the Upper Tuff of the Bapang Formation. Bars with a numeral show paleomagnetic sample horizons. Solid/open circles represent magnetic polarity of the horizon-mean paleomagnetic directions. Cross symbols indicate horizons that provide no reliable mean paleomagnetic direction. Triangular symbols indicate horizons with a transitional polarity field with a virtual geomagnetic pole (VGP) latitude of lower than 45°. LT, Lower Tuff; MT, Middle Tuff; UMT, Upper Middle Tuff; UT, Upper Tuff; UT0.5, Upper Tuff 0.5; UT1, Upper Tuff 1; UT2, Upper Tuff 2.

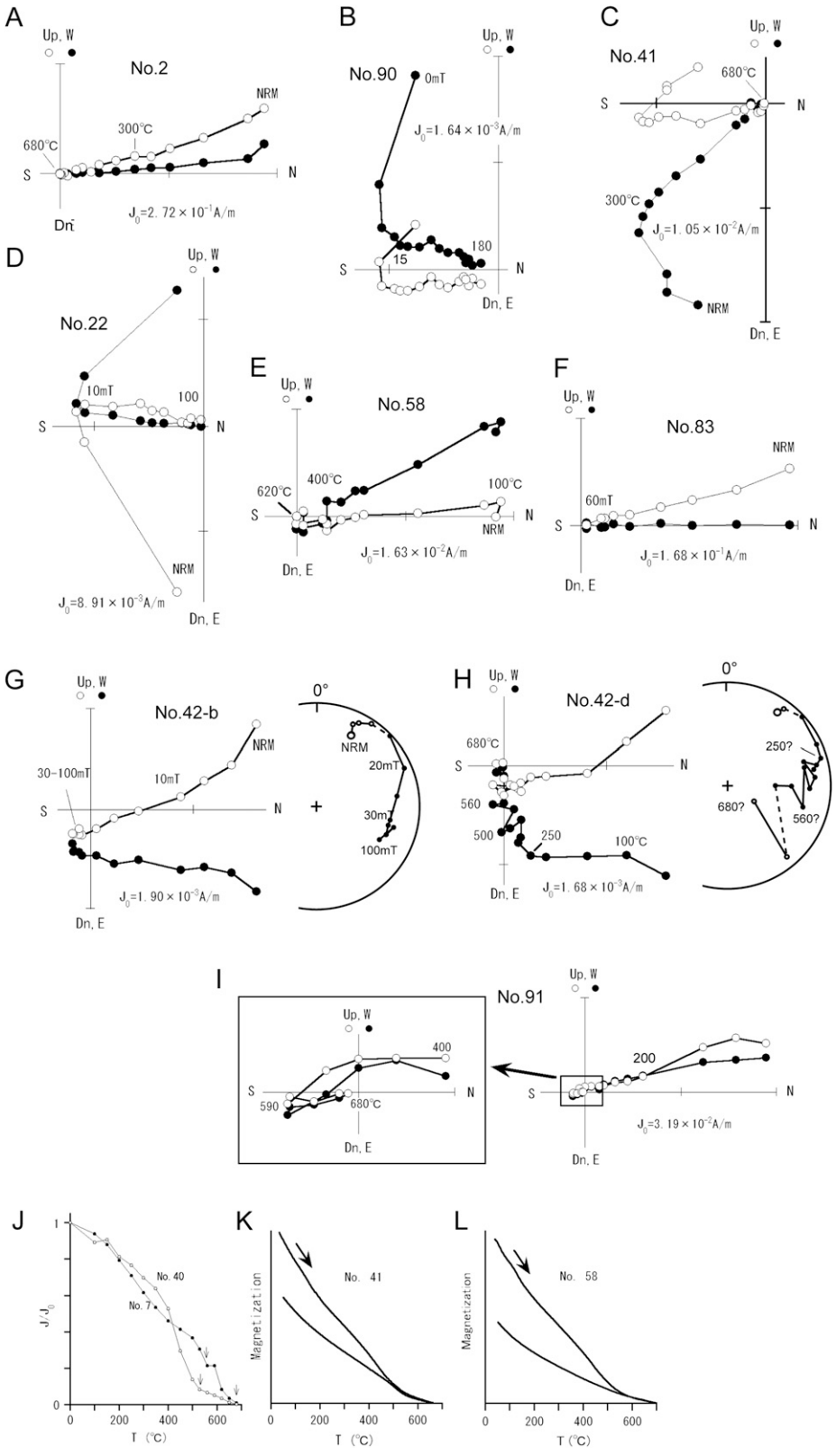

Fig. S3. Results of demagnetizations and thermomagnetic analyses. Examples of orthogonal projection diagrams and equal area projections of natural remanent magnetizations (NRMs) demagnetized thermally or in alternating fields: (*A*) Brunhes; (*B*) Matuyama; (*D–F*) short reversal episodes; (*C*, *G*, and *H*) transitional polarity fields; and (*I*) UT correlative at Pucung. Open (solid) circles represent projection on the vertical (horizontal) plane. Examples of thermal decay curves of normal polarity NRMs (*J*), and thermomagnetic analysis (JsT) results on bulk samples showing a transitional paleomagnetic direction (*K*) and a short reversal episode (*L*) during the Matuyama–Brunhes (MB) transition. Arrows in *K* and *L* show heating. For sample numbers, see Table S1.

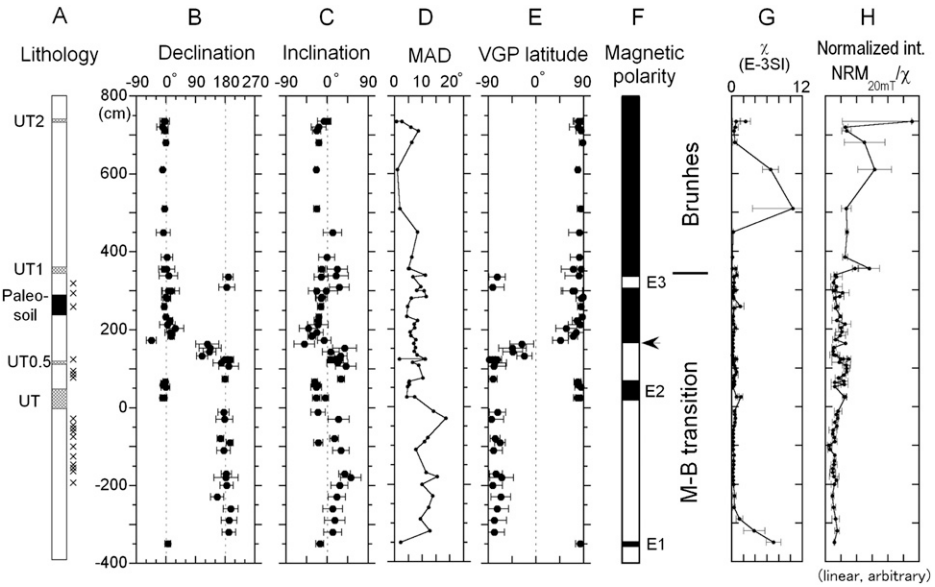

Fig. S4. Vertical plots of the combined paleomagnetic results from sections around UT of the Bapang Formation at S48 and S49 (Fig. S3). The elevation is above the base of UT at S48 (elevations at S49 are scaled to those at S48 by tuff correlations of UT, UT0.5, and UT1 and linear interpolations between them). The data below UT are all from S48, and those above UT are from both sites (Fig. S3). (*A*) Simplified lithology. Cross symbols exhibit horizons that provided no reliable mean paleomagnetic direction. Horizon mean of paleomagnetic declination (*B*), inclination (*C*), and maximum angular deviation (MAD) (*D*), and VGP latitude (*E*). Error bars show 95% confidence intervals. (*F*) Magnetic polarity defined by VGP latitude (see text). The arrow shows the main Matuyama–Brunhes boundary. E1, E2, and E3 represent short episodes. (*G*) Susceptibility. (*H*) NRM intensity demagnetized in alternating fields of 20 mT normalized by susceptibility. In *G* and *H*, data points include those for horizons that did not provide a reliable mean direction; error bars represent 1-σ intervals.

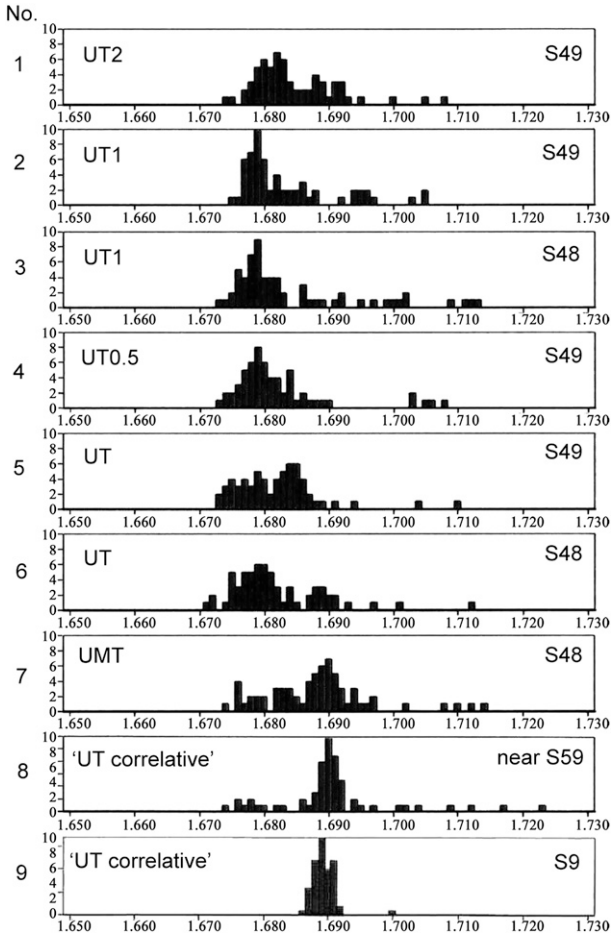

Fig. S5. Histograms of refractive indices of hornblende crystals from pinkish tuffs in the Bapang Formation.

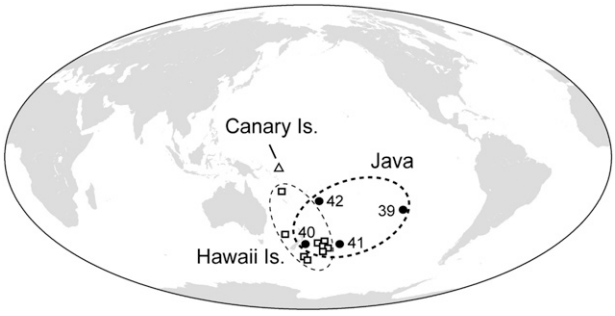

Fig. S6. Plots of VGPs of the MB transitional polarity fields. Solid circles show VGPs from Sangiran (present study). Open squares show VGPs (1) from Maui, Hawaii Islands, and one triangle, from La Palma, Canary Islands.

1. Singer BS, et al. (2005) Structural and temporal requirements for geomagnetic field reversal deduced from lava flows. *Nature* 434:633–636.

Table S1. Horizon-mean paleomagnetic direction results from the Sangiran area

Sample no.	Site	N	Dec. (°)	Inc. (°)	k	α95 (°)	VGP latitude (°)	VGP longitude (°)	MAD (°)	Demagnetization method
1	S51	5	−3.3	−1.4	37.3	12.7	82.9	83.3	8.6	T+A
2	S51	4	−3.8	−11.3	185.4	6.8	86.0	39.7	2.8	T+A
3	S43A	4	−6.3	−15.3	73.1	14.5	83.7	13.4	1.8	T+A
4	S51	5	−3.7	−17.4	21.1	20.5	85.9	−6.7	10.3	T+A
5	S43A	5	−2.0	−25.0	50.8	10.8	83.7	−56.4	3.6	T+A
6	S51	5	−5.4	−10.5	137.7	6.5	84.4	38.3	6.8	T+A
7	S43A	4	−1.0	−7.4	322.1	5.1	86.6	94.1	2.0	T+A
8	S43A	5	−1.0	−6.8	73.4	9.0	86.3	95.4	3.5	T+A
9	S43A	5	−7.6	−11.4	148.7	6.3	82.3	29.9	5.9	T+A
10	S49	5	−4.9	1.5	99.8	7.7	80.8	78.6	0.7	A
11	S49	3	−3.1	−6.6	75.3	14.3	84.8	74.3	2.7	A
12	S49	4	−9.9	−17.8	32.8	16.3	80.1	10.7	6.0	A
13	S49	3	−2.5	−22.7	193.6	8.9	85.0	−39.7	8.7	A
14	S49	3	0.5	−17.7	411.6	6.1	88.4	−86.7	6.3	A
15	S48	4	−9.7	−23.1	661.8	3.6	79.4	−5.4	1.0	T+A
16	S48	4	−3.6	−22.8	217.7	6.2	84.4	−30.4	1.9	T+A
17	S48	3	−7.5	12.5	37.9	20.3	82.5	16.3	8.4	A
18	S49	4	3.6	−0.4	29.6	17.2	82.3	139.0	6.2	T+A
19	S49	5	−4.8	−11.5	98.4	7.7	85.1	34.7	5.1	T+A
20	S48	5	3.0	22.3	14.4	22.3	70.7	119.7	5.3	T+A
21	S48	5	8.2	20.2	9.3	26.5	81.2	177.5	11.1	T+A
22	S49	3	189.8	−12.5	89.9	15.3	−73.1	−33.7	6.7	T+A
24	S49	5	185.3	26.6	20.1	21.6	−81.6	72.8	9.5	A
25	S48	4	7.5	−22.3	25.6	18.5	70.0	−90.9	8.0	T+A
26	S49	4	15.8	−1.8	14.3	25.2	73.1	−179.5	10.7	A
28	S49	5	0.3	−12.1	37.1	12.7	89.1	129.7	11.4	A
29	S49	4	3.5	−13.0	74.5	10.7	86.5	−165.6	6.1	T+A
31	S49	5	−4.6	−13.8	134.2	6.6	85.4	26.7	4.7	A
32	S49	5	0.4	−17.6	193.0	5.5	87.9	−80.1	4.5	A
33	S49	4	12.5	−20.1	133.7	8.0	77.3	−145.2	8.4	T+A
34	S49	5	5.4	−20.0	12.6	22.4	84.0	−131.0	7.2	T+A
35	S49	5	29.2	−40.6	15.7	19.9	57.8	−126.8	7.3	T+A
36	S49	5	13.3	−22.8	28.3	14.6	76.2	−139.7	5.6	T+A
37	S49	4	16.1	−33.2	111.6	8.5	70.8	−122.2	6.0	T+A
38	S49	4	−43.5	−6.0	73.8	14.7	46.5	24.3	7.7	T+A
39	S49	4	126.4	−49.8	126.4	22.4	−26.1	−119.7	7.0	T+A
40	S49	5	134.5	39.0	13.9	26.2	−43.9	177.3	7.6	T+A
41	S49	3	133.1	8.4	33.8	18.6	−43.3	−157.9	7.2	T+A
42	S49	5	110.4	30.1	33.9	14.3	−21.6	−173.7	8.2	T+A
44	S48	5	178.5	17.8	108.6	10.8	−87.8	153.2	11.0	A
45	S48	4	183.9	7.5	280.2	5.5	−81.2	−45.0	1.8	A
46	S49	5	195.9	27.4	164.2	8.8	−72.9	−46.4	11.1	T+A
47	S49	5	168.5	23.1	17.7	23.1	−77.8	178.1	6.5	T+A
48	S49	5	190.8	41.4	18.8	22.4	−79.1	33.0	8.8	T+A
52	S49	5	180.3	31.0	202.5	7.9	−80.8	109.0	10.2	T+A
53	S49	5	−1.4	−26.9	358.6	6.6	79.1	103.4	5.3	T+A
54	S48	5	−7.5	−27.1	149.2	6.3	79.9	−22.8	5.2	A
56	S49	5	−8.8	−20.8	142.1	6.4	80.7	−0.4	5.3	A
57	S48	5	−0.6	−23.6	44.4	11.6	85.1	−62.3	4.7	A
58	S49	5	−4.5	−23.6	93.4	8.0	83.5	−27.0	4.5	T+A
59	S48	4	−10.0	−4.0	161.5	7.3	78.6	49.2	7.3	A
60	S48	5	175.9	−19.5	51.5	15.7	−72.0	−82.0	14.1	T+A
62	S48	4	178.4	25.4	59.3	23.1	−83.9	125.7	18.6	A
67	S48	5	166.7	16.0	137.0	9.6	−76.8	−163.0	12.1	A
68	S48	5	194.8	−18.8	53.1	10.0	−67.4	−28.3	10.9	A
70	S48	4	175.9	30.5	100.8	17.7	−80.2	134.6	7.7	A
75	S48	5	184.3	38.7	84.0	12.3	−75.1	95.1	11.5	T+A
76	S48	5	182.7	52.4	25.2	22.6	−64.4	105.6	15.5	A
78	S48	4	185.0	27.5	37.9	18.3	−81.4	76.6	9.9	A
79	S48	5	155.9	21.3	36.1	18.8	−66.0	−169.5	13.8	A
80	S48	4	197.8	12.9	67.2	21.7	−72.7	18.8	12.4	A
81	S48	4	192.1	17.1	62.3	22.6	−78.0	27.6	9.4	A
82	S48	5	191.7	12.8	33.0	19.7	−78.4	19.1	12.8	T+A

Table S1. Cont.

Sample no.	Site	N	Dec. (°)	Inc. (°)	k	α95 (°)	VGP latitude (°)	VGP longitude (°)	MAD (°)	Demagnetization method
83	S48	4	6.0	−15.4	118.7	8.5	84.0	−155.5	2.3	A
84	S48	5	176.5	−26.8	56.0	11.7	−68.0	−78.3	13.3	T+A
85	S48	5	177.7	13.0	95.7	11.5	−87.5	−137.5	8.1	T+A
86	S48	5	170.0	−7.7	13.2	26.9	−74.9	−110.8	9.9	T+A
87	S48	3	178.9	7.5	245.6	7.9	−86.1	−85.6	3.9	T+A
89	S48	4	167.3	25.0	61.4	11.8	−76.3	175.5	2.8	A
90	S48	5	192.2	14.8	23.0	16.3	−77.9	22.0	9.6	T+A
91	S59	5	182.0	3.4	28.8	14.9	−83.9	−50.1	7.0	T+A
92	S9	4	191.3	32.8	37.1	29.4	−74.9	65.1	12.7	A

A representative global positioning system position within the sampling tract shown by red arrows in Fig. 1 is S7°28.341, 110°51.777′ (S51), S7°29.201′, E110° 51.258′ (S43A), S7°28.032′, 110°51.434′ (S49), S7°, 27.943′, E110°51.395′ (S48), S7°28.875′, E110°51.011′ (S59), and S7°28.461′, E110°51.033′ (S9). A, alternating field demagnetization; α95, radius of 95% confidence circle; Dec, declination; Inc, inclination; k, precision parameter; MAD, maximum angular deviation; N, number of specimens; T, thermal demagnetization.

Table S2. Results of analyses for pinkish tuff layers

No.	Tuff	Site	Heavy minerals	Hb min–max (mode); mean ± SD
1	UT2	S49	GHb,Opq > BHb	1.674–1.695 (1.682); 1.684 ± 0.005
2	UT1	S49	Opq,GHb > BHb	1.675–1.687 (1.679); 1.681 ± 0.003
3	UT1	S48	GHb > Ap,Opq,BHb	1.673–1.683 (1.679); 1.679 ± 0.003
4	UT0.5	S49	GHb,Opq,BHb > Ap	1.673–1.690 (1.679); 1.680 ± 0.004
5	UT	S49	GHb,Opq > Bt,BHb,Ap	1.673–1.694 (1.684–1.685); 1.681 ± 0.005
6	UT	S48	>Opq,GHb	1.671–1.693 (1.679–1.680); 1.681 ± 0.006
7	UMT	S48	GHb,Opq > BHb,Ap,Opx	1.674–1.697 (1.690); 1.687 ± 0.006
8	UT	S59	GHb > Opq,Cpx,BHb	1.686–1.697 (1.690); 1.690 ± 0.002
9	UT	S9	GHb > Opq > BHb,Ap	1.686–1.692 (1.689)

Tuffs: UT2, UT1, and UT0.5 are newly defined (see text). UT and UMT are after Itihara et al. (1). Sites: S48 and S49, Bapang; S59, Pucung; S9, Tanjung. Heavy minerals: Ap, apatite; BHb, brown hornblende; Bt, biotite; Cpx, clinopyroxene; GHb, green hornblende; Opq, opaque minerals; Opx, orthopyroxene.

1. Itihara M, et al. (1985) Geology and stratigraphy of the Sangiran area. *Quaternary Geology of the Hominid Fossil Bearing Formations in Java,* eds Watanabe N, Kadar D (Geological Research and Development Centre, Bandung, Indonesia), pp 11–43.